Role of Nitric Oxide in Angiogenesis and Tumor Progression in Head and Neck Cancer

*Oreste Gallo, Emanuela Masini, Lucia Morbidelli, Alessandro Franchi, Isabella Fini-Storchi, William A. Vergari, Marina Ziche**

Background: **Angiogenesis (formation of new blood vessels) is associated with tumor growth and metastasis in patients with solid tumors, including those of the head and neck. Nitric oxide (NO) production may contribute to these processes. We assessed the role of the NO pathway in angiogenesis and tumor progression in patients with head and neck cancer.** ***Methods:*** **Biochemical assays were used to measure NO synthase (NOS) activity and cyclic guanosine monophosphate (cGMP) levels in specimens of tumor and normal mucosa obtained from 27 patients. Microvessels in tumor specimens were identified by CD-31-specific immunohistochemical staining. Associations between microvessel densities, levels of NOS, and cGMP were examined by use of two-sided statistical tests. Tumor specimens and human squamous carcinoma A-431 cells were grown as explants on the corneas of rabbits, and the effect of the NOS inhibitor N^{ω}-nitro-L-arginine-methyl ester (L-NAME) was tested.** ***Results:*** **Levels of total NOS, inducible NOS, and cGMP were higher in tumor specimens than in specimens of normal mucosa (all $P<.0001$). Tumor specimens from patients with lymph node metastases presented a higher total NOS activity ($P = .005$) and were markedly more vascularized than tumor specimens from patients with no lymph node involvement ($P = .0002$). Microvessel density at the tumor edge was an independent predictor of metastasis for this series of patients (odds ratio = 1.19; 95% confidence interval = 1.07–2.89; $P = .04$). A-431 cells and tumor specimens exhibiting high levels of NOS activity induced angiogenesis in the rabbit cornea assay; when NO production was blocked, tumor angiogenesis and growth were repressed.** ***Conclusions:*** **The NO pathway appears to play a key role in tumor angiogenesis and spread in patients with head and neck cancer. [J Natl Cancer Inst 1998;90:587–96]**

Squamous cell carcinoma of the head and neck is among the most common human cancers and remains a major cause of mortality and morbidity throughout the world *(1).* The most

**Affiliations of authors:* O. Gallo, I. Fini-Storchi, W. A. Vergari (Institute of Otolaryngology Head and Neck Surgery), E. Masini, L. Morbidelli, M. Ziche (Department of Preclinical and Clinical Pharmacology), A. Franchi (Institute of Anatomic Pathology), University of Florence, Italy.

Correspondence to: Marina Ziche, M.D., Department of Pharmacology, University of Florence, Viale Morgagni 65, 50134 Florence, Italy. E-mail: ziche@stat.ds.unifi.it

See ''Notes'' following ''References.''

important prognostic factor in patients with head and neck cancer is the presence of lymph node metastasis that correlates with locoregional recurrence, distant metastatic spread, and survival *(2).* As documented in both clinical and experimental studies [reviewed in *(3)*], the ability of tumor cells to induce new blood vessel growth (angiogenesis) is a critical factor in determining tumor size as well as regional and distant tumor spread. If tumor angiogenesis is limited or prevented, tumor cells are much more likely to undergo programmed cell death (apoptosis) and tumor growth is strongly reduced. On the basis of the hypothesis that inhibition of angiogenesis results in a reduction of tumor size and metastases, several antiangiogenic drugs are presently under investigation as new therapeutic strategies in cancer treatment *(4,5).*

Head and neck squamous cell carcinomas have been found to promote microvascular growth *in vivo.* Culture supernatants from head and neck squamous cell carcinoma cell lines grown *in vitro* have also been found to promote microvascular growth in the chorioallantoic membrane (angiogenesis) assay *(6,7).* The density of microvessels in head and neck tumors has consistently been found to correlate with metastatic spread and prognosis *(8–10).* However, no information is available to date regarding the nature of the angiogenic mediator implicated.

Immunohistochemical studies *(11–13)* have indicated that nitric oxide (NO) synthase (NOS) is present at higher levels in solid tumors, including those of the head and neck, compared with normal tissue *(11–13);* however, no definite explanation for the role of NO in tumor growth has been provided *(14).* NO functions as a mediator in the vascular, nervous, and immune systems by regulating vasodilation, vascular permeability, platelet adhesion and aggregation, and tumor blood flow *(15–17).* We recently reported *(18,19)* that NO plays a central role in the angiogenic cascade by demonstrating that vascular endothelial growth factor (VEGF), released as a purified protein or produced by tumor cells, requires a functioning NO/cyclic guanosine monophosphate (cGMP) pathway within the endothelial compartment to promote neovascular growth.

We pursued the hypothesis that the NO pathway could control the sequential steps responsible for the neovascularization in head and neck cancer and thus influence tumor cell dissemination. To this aim, we have assessed the status of the NOS/cGMP pathway and its association with microvessel density in a series of 27 head and neck cancer patients distributed according to lymph node status. The ability to directly stimulate angiogenesis by head and neck cancer was assessed *in vivo* in the avascular cornea of albino rabbits. The role of NO in controlling angiogenesis was evaluated *in vivo* in rabbits receiving pharmacologic inhibition of NOS pathway produced by N^{ω}-nitro-L-arginine-methyl ester (L-NAME). The effect of the treatment was evaluated for its ability to prevent angiogenesis and to produce its regression in animals implanted with tumor tissue and with a squamous cell carcinoma cell line.

Materials and Methods

Patients and Tissue Collection

We studied 27 consecutive head and neck cancer patients who underwent surgical treatment of the primary tumor and of the neck at the Institute of Otolaryngology Head and Neck Surgery, University of Florence, during the period from April 1996 through April 1997. Clinical, epidemiologic, and histopathologic characteristics of these patients are shown in Table 1. All tumors were histologically confirmed to be squamous cell carcinomas and were graded as well differentiated, moderately differentiated, and poorly differentiated *(20,21).*

Samples of the tumor core, the invasive edge of the tumor (tumor edge), and macroscopically healthy mucosa (control) were obtained from surgical specimens taken from each patient for NO analysis and angiogenesis assay. The portion of primary tumor was obtained by superficial biopsy of either the tumor bulk or the edge of the malignant ulcer for more infiltrative cancers. Samples of tissue identified as tumor edge were taken at the tumor periphery, whereas samples of control mucosa were obtained from a macroscopically uninvolved area 2–5 cm away from the tumor.

Cell Line and Culture Conditions

Human epidermoid carcinoma A-431 cells were obtained from the American Type Culture Collection (Rockville, MD). Cells were maintained in culture in Dulbecco's modified Eagle medium supplemented with 4500 g/L glucose, 2 m*M* L-glutamine, antibiotics (100 U/mL penicillin and 100 μg/mL streptomycin) (Sigma Chemical Co., St. Louis, MO), and 10% fetal calf serum (FCS) (Hyclone Laboratories, Inc., Logan, UT). Cells were split 1 : 5 twice a week.

Assay for NOS Activity

Fragments of tissues were homogenized at 0–4 °C in buffer containing 0.32 *M* sucrose, 20 m*M* HEPES (pH 7.2), 0.5 *M* EDTA, and 1 m*M* dithiothreitol. The homogenates were then processed, and the total NOS (tNOS) activity was measured as previously described *(22).* The activity of the calcium-calmodulin-independent isoform (inducible NOS [iNOS]) was identified in tumor homogenates by measuring the enzymatic activity in buffer containing 1 m*M* EGTA and the calmodulin inhibitor trifluoperazine (100 μ*M*) (but no calcium) as previously reported *(22).* For the evaluation of NOS activity in A-431 cells, the cells in 60-mm-diameter culture dishes were stimulated with 10 μg/mL lipopolysaccharide (LPS) for 24 hours and treated as described *(23).* All determinations were performed in duplicate. NOS activity is expressed as picomoles of [^{3}H]citrulline formed per minute per milligram protein.

Measurement of cGMP Content

The levels of cGMP were measured in the aqueous phase of tissue homogenates extracted from 10% trichloroacetic acid with 0.5 *M* tri-*n*-octylamine dis-

Table 1. Clinical, epidemiologic, and histologic characteristics of 27 patients with squamous cell carcinoma of the head and neck

Characteristic	No. (%)
Total No. of patients	27 (100)
Age, y	
Median: 64	
Range: 43–75	
Sex	
Male	23 (85.1)
Female	4 (14.9)
Tumor stage *(20)*	
I	4 (14.9)
II	5 (18.5)
III	7 (25.9)
IV	9 (33.3)
Recurrences	2 (7.4)
Tumor site	
Larynx	18 (66.7)
Oral cavity	6 (22.2)
Oropharynx	3 (11.1)
Lymph node status	
Negative (N−)	16 (59.3)
Positive (N+)	11 (40.7)
Tumor grade *(21)*	
Well-differentiated	9 (33.3)
Moderately differentiated	12 (44.5)
Poorly differentiated	6 (22.2)

solved in 1,1,2-trichlorotrifluoroethane *(22).* cGMP was measured with the use of a radioimmunoassay kit and ^{125}I-labeled cGMP (Amersham, Buckinghamshire, England) after acetylation of the samples with acetic anhydride. All determinations were performed in duplicate. Values are expressed as femtomoles of cGMP per milligram protein.

Immunofluorescence Analysis of Inducible Form of NOS

Tissue samples were frozen by immersion in liquid nitrogen, and 7-μm-thick sections were cut with the use of a cryostat. A-431 cells were grown on multichamber glass slides coated with gelatin. Both the sections and the cell specimens were fixed in 4% formaldehyde in phosphate-buffered saline (PBS) for 10 minutes at room temperature, washed thoroughly in PBS, and then immunolabeled with rabbit polyclonal anti-iNOS antibodies (Calbiochem, Inalco, Milan, Italy; working dilution 1 : 25). The immune reaction was detected with fluorescein isothiocyanate-labeled goat anti-rabbit serum (Sigma Chemical Co.; working dilution 1 : 40). The immunostained sections were mounted in Gel-mount (Biomeda, Foster City, CA) and then observed and photographed under an Axioskop UV light microscope (Zeiss, Oberkochen, Germany).

Microvessel Density Determination

Microvessels were identified in formalin-fixed, paraffin-embedded tumor tissue sections by use of an immunohistochemical method. A monoclonal antibody against CD-31 (JC/70; Dako, Glostrup, Denmark) diluted at 1 : 20 in PBS was employed. Incubation was carried out for 30 minutes, after digestion of the tissue sections with protease XIV (Sigma Chemical Co.) for 3 minutes at 37 °C. Sections were stained with use of a standard streptavidin–avidin–biotin technique (LSAB kit; Dako) with diaminobenzidine as chromogen and hematoxylin as counterstain. Microvessel density was determined by use of the procedure proposed by Weidner et al. *(24).* The tumor area with the highest concentration of stained microvessels was identified at scanning magnification (×40), and microvessels were counted in a blinded manner by two independent operators at ×200 magnification (field area, 0.73 mm^2). Results are expressed as the highest number of microvessels identified within a ×200 field.

Rabbit Cornea Assay for Angiogenesis

Corneal assays for angiogenesis were performed in New Zealand white rabbits (Charles River, Calco, Como, Italy) as described *(25)* and in accordance with the guidelines of the European Economic Community (EEC) for animal care and welfare (EEC law No. 86/609). Tumor fragments (2–3 mg each) or cell suspensions (2.5×10^5 cells) were implanted into surgically produced corneal micropockets. The angiogenic response was assessed in a blinded manner by two independent operators, who did not perform the surgery, by use of a slit lamp stereomicroscope, and capillary progression was scored daily as previously reported *(26).* The number of tissue samples inducing angiogenesis over the total number of implants performed was recorded during each observation. Implants that failed to produce a neovascular growth within 10 days were considered negative, while implants showing an inflammatory reaction were discarded. The potency of angiogenic activity (angiogenic score) was determined on the basis of the number and growth rate of newly formed capillaries and calculated as vessel density × distance from the limbus *(19,27).* Corneas were removed at the end of the experiment as well as at defined intervals after surgery and/or treatment and were fixed in formalin for histologic examination.

To evaluate the effect of NOS inhibition on tumor angiogenesis, we administered L-NAME in the drinking water. L-NAME solutions (1 g/L) were freshly prepared every day. Water intake was approximately 200 mL/day per animal in the treated animals and was not different from that in animals in the control group. After 14 days of treatment and after 5 days from the end of treatment, rabbits were killed and autopsied. L-NAME was shown to have effectively inhibited NOS activity in the rabbits by evaluation of the contractility of the aortic rings *(27).*

Differential Reverse Transcription–Polymerase Chain Reaction Analysis of NOS Expression

A-431 cells at 90% confluence were stimulated for 24 hours with test substances in the presence of 1% FCS. Total RNA from cells was isolated by the standard guanidinium thiocyanate-phenol-chloroform extraction *(28).* Complementary DNA (cDNA) was synthesized as described *(29).* Differential reverse transcription–polymerase chain reaction (RT–PCR) *(29)* for NOS isoforms was carried out by use of 5 μL of cDNA and specific primers with sequences as follows: for endothelial NOS (eNOS), sense 5′-GTG ATG GCG AAG CGA GTG AAG-3′, antisense 5′-CCG AGC CCG AAC ACA CAG AAC-3′; for iNOS, sense 5′-TCC GAG GCA AAC AGC ACA TTC A-3′, antisense 5′-GGG TTG GGG GTG TGG TGA TGT-3′ *(30).* Calibration was performed by coamplification of the same cDNA sample with primers for glyceraldehyde 3-phosphate dehydrogenase (GAPDH) as internal standard, with sequences as described *(29).* The PCR cycles were 1 minute at 94 °C, 1 minute at 60 °C, and 1.5 minutes at 72 °C for eNOS and iNOS. After 35 cycles of amplification, aliquots of each sample product (20 μL) were subjected to electrophoresis on a 3% agarose gel and stained with ethidium bromide. The size of the amplification products were 196 base pairs (bp) for GAPDH, 422 bp for eNOS, and 462 bp for iNOS. Image processing and analysis of the intensity of the bands were performed as described *(29).* The results were analyzed as the ratio between the optical densities of the bands related to the amplification products of the target genes (eNOS and iNOS) and GAPDH.

Statistical Analysis

Statistical analysis was performed with use of Stata Statistic Software (release 5.0; Stata Corporation, College Station, TX) and Number Cruncher Statistical System (version 5.03; J. L. Hintze, Kaysville, UT). Data are reported as median and range for NOS/cGMP values and microvessel density and as means with 95% confidence intervals (CIs) for the angiogenesis score.

Within different tissue samples, NOS activity and cGMP levels were compared by use of a paired-value Wilcoxon test. The Wilcoxon rank sum test for unpaired data was used to assess the differences between NOS activity and cGMP levels in different tissues as well as microvessel density (CD-31 staining) according to lymph node status.

The relationships between the microvessel count and NOS activity and cGMP levels are reported as Spearman product-moment correlation coefficient (r_S). Moreover, differences among microvessel density according to tumor stage and tumor grade were analyzed by the use of the Kruskal–Wallis test.

A multivariate logistic regression analysis was performed to explore the effects of several possible prognostic factors (age, sex, tumor grade, tumor stage, tumor location, microvessel density, NOS activity, and cGMP levels) in predicting the risk of lymph node metastases. The final results of these analyses are the odds ratios (ORs) and their 95% CIs. The Wald statistic was used to test the following hypothesis: OR = 1.00.

For the angiogenesis data, multiple comparisons were performed by analysis of variance (ANOVA), and individual differences during each day of observation were tested by Fisher's test after the demonstration of significant intergroup differences by ANOVA.

All *P* values resulted from use of two-sided statistical tests. *P* values less than .05 were considered to indicate statistically significant differences.

Results

NOS Activity in Normal and Neoplastic Tissues of the Upper Aerodigestive Tract: Correlation With Lymph Node Metastasis

The activities of tNOS and iNOS were measured in biopsy specimens obtained from the tumor core, the invasive edge of the tumor (tumor edge), and normal mucosa in 27 patients who underwent surgery for head and neck cancer.

In specimens from unaffected mucosa, we detected a median baseline activity of tNOS and iNOS of 1.37 (range, 0.64–3.50) and 0.95 (range, 0.59–2.93) pmol/minute per mg protein, respectively. In tumor tissue, tNOS and iNOS levels were elevated to 4.08 (range, 2.03–8.78) and 3.67 (range, 1.94–6.85) pmol/minute per mg protein, respectively (paired-value Wilcoxon test, $P<.0001$ in all cases compared with normal control mucosa). The localization of NOS enzyme within the tumor cell population was assessed by immunofluorescence analysis on tumor sections by the use of polyclonal anti-iNOS antibodies. The strongest immunoreactivity was detected in cancer cells rather than in stromal cells. In normal control mucosa, the iNOS im-

munostaining was prevalent in the epithelial cells of the basal layer (Fig. 1, A and B).

The extent of NOS activity increment was significantly different according to the site of sampling within the tumor mass. The specimens at the invasive edge of the tumor exhibited the highest NOS activity. In tumor core samples, the median value was 4.08 (range, 2.03–8.78) pmol/minute per mg protein for tNOS and 3.67 (range, 1.94–6.85) pmol/minute per mg protein for iNOS; in samples from the tumor edge, the values were 5.36 (range, 2.73–23.74) pmol/minute per mg protein for tNOS and 4.06 (range, 2.04–21.83) pmol/minute per mg protein for iNOS (paired-value Wilcoxon test, tumor core versus tumor edge: $P = .0003$ for tNOS and $P = .004$ for iNOS activity, respectively).

We then analyzed NOS activity in tumor specimens from patients in the cohort according to tumor stage and metastatic behavior. Eleven patients had histologically confirmed cervical lymph node metastases (N+), whereas the remaining 16 patients had no clinical and histopathologic evidence of neck disease (N−). The levels of NOS in specimens from N+ patients were higher in each tissue sample examined compared with the specimens sampled from patients with histologically negative (i.e., no detectable cancer) lymph nodes (Fig. 2, A and B).

Accordingly, the specimens sampled at the periphery of the tumor had significantly higher tNOS and iNOS activities in more advanced disease (stage III or IV) *(20)* when compared with those from early stage lesions (stage I or II) ($P = .016$ and $P = .04$, respectively). No difference in the levels of tNOS and iNOS activities in specimens was found according to tumor grade.

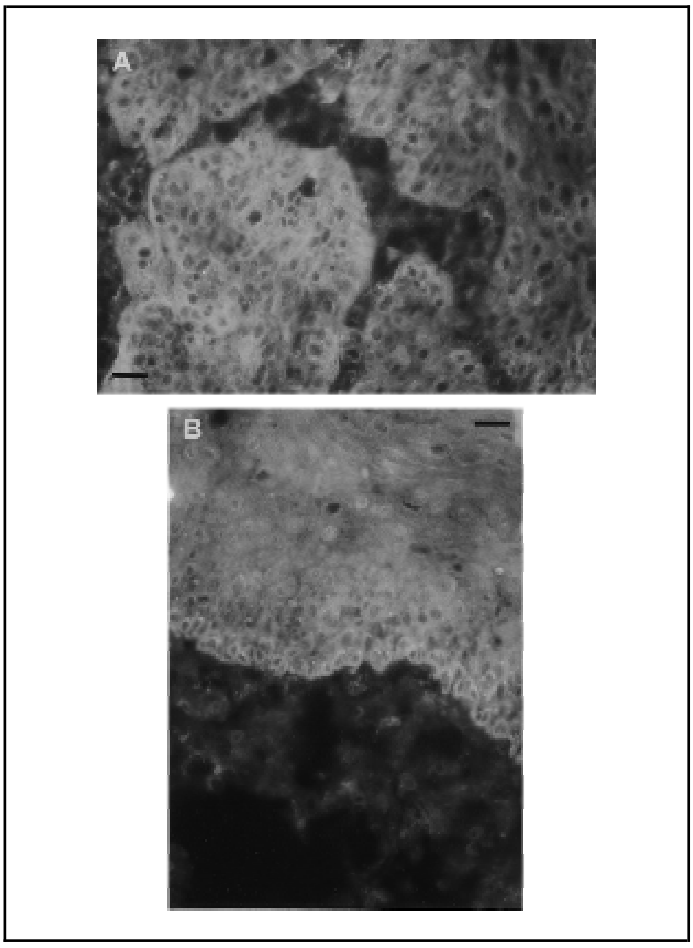

Fig. 1. Nitric oxide synthase (NOS) expression in tumor samples and normal mucosa from head and neck cancer patients. A representative picture is shown of immunofluorescence detection of inducible NOS in cancer tissue **(A)** and in normal control mucosa **(B).** Tissues were obtained from patients who underwent surgery for head and neck cancer (original magnification ×500; bar = 20 μm).

cGMP Determination in Normal Mucosa and Tumor Tissue: Correlation With Lymph Node Metastasis

cGMP is known to be the mediator of the response of the cells to NO *(31).* To ascertain whether cGMP undergoes changes in head and neck cancers, we next measured cGMP levels in the aqueous phase of 10% trichloroacetic acid extracts of head and neck cancer tissues. Increased cGMP levels were detected in the tumor core and the tumor edge (median values of 5.39 [range, 3.35–7.93] and 6.37 [range, 3.84–16.81] fmol/mg protein, respectively) compared with normal control tissues (2.97 [range, 1.87–4.96] fmol/mg protein) (paired-value Wilcoxon test, $P<.0001$). The increment of cGMP levels in the tumor edge was significantly higher than in the tumor core (paired-value Wilcoxon test, $P = .0001$). When cGMP levels in tissues from N+ patients were compared with those from N− patients, a statistically significant difference was demonstrated only in the tumor edge (unpaired-value Wilcoxon test, $P = .005$) but not in unaffected control mucosa ($P = .805$) or in the tumor core ($P = .621$) (Fig. 2, C).

A progressive increase in cGMP was also detected from stage I to IV tumors only in peritumoral samples, although this finding was not statistically significant ($P = .156$). No difference in cGMP levels was found according to tumor grade.

Correlation of Microvessel Density With NOS Activity, cGMP Levels, Lymph Node Status, Tumor Grade, and Tumor Stage: Multivariate Analysis

We then assessed the extent of vascularization in our series of head and neck cancer patients. Immunohistochemical expression of CD-31 and Ki-67 was detected as previously described *(32).* Microvessel counts in cancers from different patients and also within different areas of the same carcinoma were heterogeneous. The highest density of microvessels was observed at the invasive edge of the tumor and was associated with an increased proliferative activity of tumor cells (Fig. 3). According to tumor grade, we found a statistically significant increase in the microvessel counts passing from well-differentiated to poorly differentiated carcinomas (Spearman coefficient $r_S = .435$; $P = .03$), as well as from early stage cancers to more advanced cancers ($r_S = .599$; $P = .001$). N+ patients had a significantly higher median microvessel count in tumor specimens than N− patients (unpaired-value Wilcoxon test, $P = .0002$) (Fig. 3).

When we correlated tNOS and iNOS activities with microvessel density in the tumor core and tumor edge samples, we found that the increased tumor vascularization was statistically associated with an increased NOS activity (both tNOS and iNOS) ($r_S = .468$ and $P = .016$ and $r_S = .434$ and $P = .027$ in tumor core, respectively; $r_S = .571$ and $P = .002$ and $r_S = .498$ and $P = .010$ in tumor edge, respectively). A suggestive correlation between cGMP activity and CD-31 density was ob-

served only in samples from the tumor periphery (r_S = .352; P = .078). Furthermore, analysis indicated that there was a statistically significant association between vascular density and tumor stage (Kruskal–Wallis test; P = .018).

Thus, increased NOS activity and cGMP levels in both the tumor core and the tumor-front areas, high microvessel density, and poor histologic differentiation of cancers were significantly correlated with the presence of lymph node metastasis. Multivariate stepwise logistic regression analysis confirmed that microvessel count (CD-31 expression) was the most important and independent predictor of lymph node metastasis in our series (OR = 1.19; 95% CI = 1.07–2.89; Wald statistic = 3.79; P = .04), whereas cGMP levels were strongly suggestive (OR = 1.39; 95% CI = 0.97–1.99; Wald statistic = 1.79; P = .06).

Angiogenesis Produced by Head and Neck Cancer Tissue: Blockage by NOS Inhibitor

To assess whether the tumor expression of NOS activity could be directly correlated with an increased angiogenic potential, we assayed tumor specimens of head and neck cancer for angiogenesis in an *in vivo* experimental setting by use of the avascular rabbit cornea to monitor vascular growth. Fragments (2–3 mg) of tumor tissue and of unaffected control mucosa from 12 randomly selected patients with either positive (five patients) or negative (seven patients) lymph nodes were sampled and implanted in the corneal stroma. For each specimen, at least two fragments were tested. Within 5 days from the implant, all tumor fragments induced a strong angiogenic response in all the re-

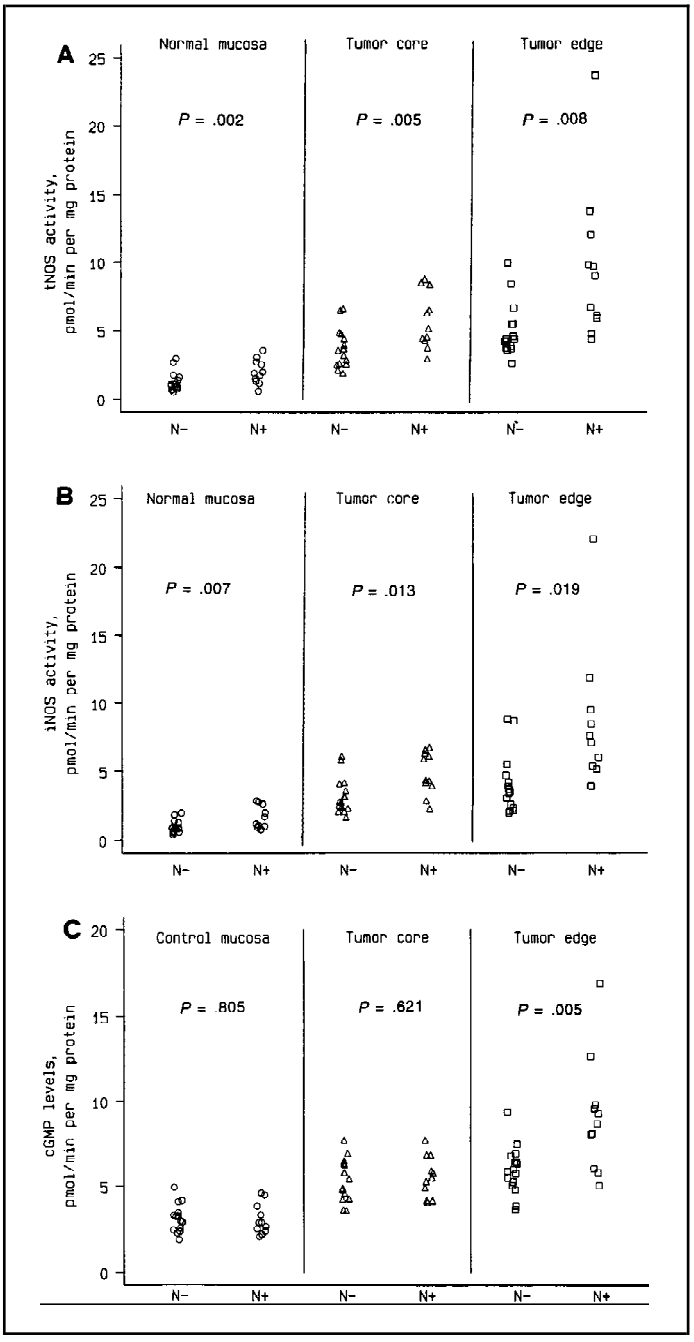

Fig. 2. Nitric oxide synthase (NOS) activity and cyclic guanosine monophosphate (cGMP) levels in tumor samples and normal mucosa from head and neck cancer patients. Total NOS (tNOS) **(A)** and inducible NOS (iNOS) **(B)** activities were measured in specimens selected from the tumor core, the invasive edge of the tumor (tumor edge), and normal mucosa (control). Data are expressed as pmol of [^{3}H]citrulline formed/minute per mg protein. tNOS and iNOS activities are sorted and compared according to lymph node status (11 lymph node-negative [N−] and 16 lymph node-positive [N+] patients). tNOS activities for control mucosa, tumor core, and tumor edge were 0.95 (range, 0.64–2.67), 3.62 (range, 2.03–6.54), and 4.37 (range, 2.73–9.72) pmol/minute per mg protein, respectively, for N− patients and 1.93 (range, 0.96–3.50), 4.96 (range, 2.79–8.78), and 8.97 (range, 4.61–23.74) pmol/minute per mg protein, respectively, for N+ patients. iNOS activities for control mucosa, tumor core, and tumor edge specimens were 0.81 (range, 0.59–2.16), 2.70 (range, 1.94–6.07), and 3.68 (range, 2.041–8.98) pmol/minute per mg protein, respectively, for N− patients and 1.10 (range, 0.63–2.93), 4.07 (range, 2.04–6.85), and 6.98 (range, 3.89–21.83) pmol/minute per mg protein, respectively, for N+ patients. **C)** cGMP levels were measured in the aqueous phase of tissue homogenates by radioimmunoassay. Data are expressed as fmol/mg of protein (11 N− and 16 N+ patients). cGMP levels in control mucosa, tumor core, and tumor edge were 3.01 (range, 2.02–4.96), 5.21 (range, 3.35–7.42), and 5.96 (range, 3.846–9.41) pmol/mg protein, respectively, for N− patients and 2.73 (range, 1.87–4.71), 5.63 (range, 3.91–7.93), and 8.52 (range, 4.96–16.81) pmol/mg protein, respectively, for N+ patients.

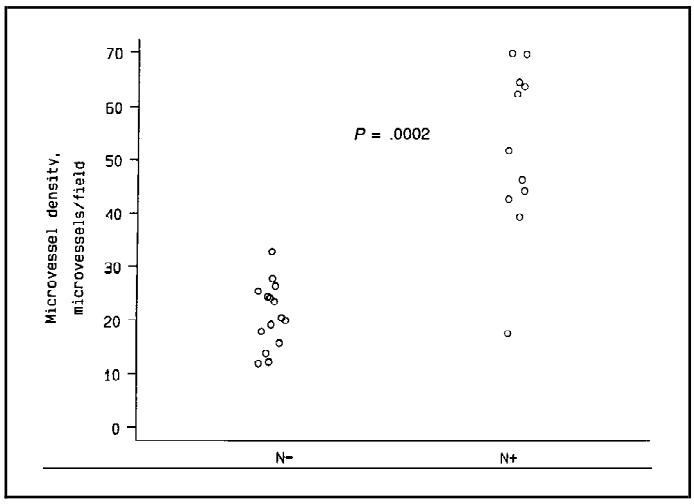

Fig. 3. Microvessel density in head and neck cancer according to lymph node status. The immunohistochemical staining was performed as described in the ''Materials and Methods'' section. Results are expressed as the highest number of microvessels identified within a ×200 field (11 lymph node-negative [N−] and 16 lymph node-positive [N+] patients). Median microvessel density was 21 microvessels per field (range, 12–32) and 52 microvessels per field (range, 18–70) for N− and N+ patients, respectively.

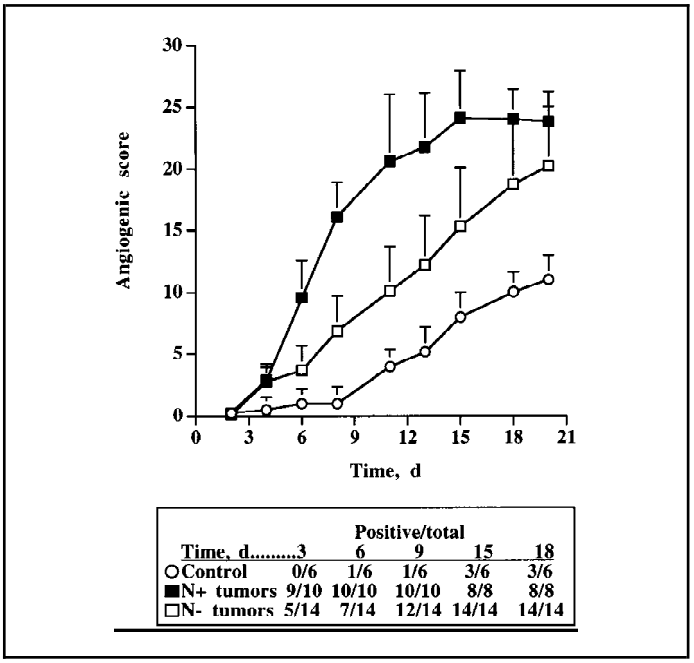

Time, d.....3	Positive/total 6	9	15	18
○Control 0/6	1/6	1/6	3/6	3/6
■N+ tumors 9/10	10/10	10/10	8/8	8/8
□N- tumors 5/14	7/14	12/14	14/14	14/14

Fig. 4. Angiogenesis produced in the rabbit cornea by normal control mucosa and tumor specimens from head and neck cancer patients. Progression and efficiency over time of neovascular growth produced by nonpathologic mucosa and tumor tissue from head and neck cancer patients according to lymph node status. Angiogenesis is reported as angiogenic score (vessel length × vessel density) over time (days). In the inset is reported the number of tissue samples inducing angiogenesis over the total number of samples tested (positive/total). One animal bearing two samples was killed because of tumor overgrowth. The sample size consisted of six samples from three patients for normal mucosa, 14 samples from seven lymph node-negative (N−) patient tumors, and 10 samples (until day 10) from five lymph node-positive (N+) patient tumors. d = day.

cipient animals, whereas only a few of the implanted fragments elicited a modest angiogenic response (Fig. 4; Fig. 5, a). In the following days (days 12–15), angiogenesis induced by the tumors progressed; the newly formed capillaries reached the tumor implant, vascularized it, and produced an increase in the tumor size (Fig. 4; Fig. 5, a–c). Samples from N+ patients (14 fragments from seven patients) induced a more potent angiogenic response than samples from N− patients (50% increase in neovascularization, 10 fragments from five patients) (Fig. 4). Fisher's test after ANOVA analysis revealed a statistically relevant difference between the three groups from day 8 to day 18 of observation ($P = .01$).

To assess whether head and neck cancer-induced angiogenesis could be controlled by NOS inhibition, two experimental approaches were followed. In a first set of experiments, a group of animals received the NOS inhibitor L-NAME (1 g/L) in the drinking water once a consistent vascular network had been elicited by the tumor implant in the cornea (Fig. 5, c). By 24 hours after the administration of the NOS inhibitor, the diameters of the capillaries, measured by use of an ocular grid, were reduced by 50%, thus resulting in decreased tumor perfusion. In the following days, the vascular network started to regress (Fig. 6, A) (Fisher's test following ANOVA; $P = .05$), while the tumor size appeared grossly reduced (about 50% reduction) (Fig. 5, d–f; Fig. 6, A). Conversely, the tumor fragments in the control group did not change their size or vascular support.

In a second set of experiments, L-NAME treatment was given before the animals received the tumor implant. Under systemic inhibition of NOS activity in the host, angiogenesis was not produced by any implanted tumor samples (zero vascularized implants of eight performed in L-NAME-treated animals versus six of eight in untreated rabbits) (Fisher's test following ANOVA, $P = .01$ for days 8–18) (Fig. 6, B). When the treatment was interrupted, vascularization started from the 8th day after the suspension of treatment and progressed, reproducing the vascular pattern of untreated, implanted animals (Fig. 6, B).

Control by NO of Angiogenesis by Squamous Cell Carcinoma Cell Line A-431

To prove that the NO production by the neoplastic cell population triggered angiogenesis, we used the epidermoid cell line A-431 as an experimental tumor model. This cell line was characterized for NOS isoform activity and for NO production and was assessed in the rabbit cornea angiogenesis assay.

The extent of NO produced under basal conditions was approximately 3.8 (95% CI = 3.0–4.6) pmol/minute per mg protein. Immmunofluorescence analysis revealed a clear-cut cytoplasmic localization of iNOS immunostaining (data not shown). By differential RT–PCR, the constitutive presence of two NOS isoforms was shown, identifiable with the eNOS and the iNOS isoforms (mean ratios of 0.380 [95% CI = 0.351–0.409] and 0.341 [95% CI = 0.327–0.355] for eNOS and iNOS, respectively). NO production by A-431 cells could be modulated. Following a 24-hour stimulation with 10 μg/mL LPS, the NOS activity increased by approximately threefold (10.71 [95% CI = 9.45–11.97] pmol/minute per mg protein in LPS-treated cells [$P<.001$] versus basal control, Student's *t* test), an effect that could be specifically blocked by L-NAME (3.04 [95% CI = 2.56–3.52] pmol/minute per mg protein in cells treated with 2 m*M* L-NAME [$P<.01$] versus LPS alone, Student's *t* test).

A-431 cells treated *in vitro* for 24 hours with LPS (10 μg/mL) and then implanted in the cornea elicited angiogenesis within 5 days, and complete vascularization of the tumor cell implant

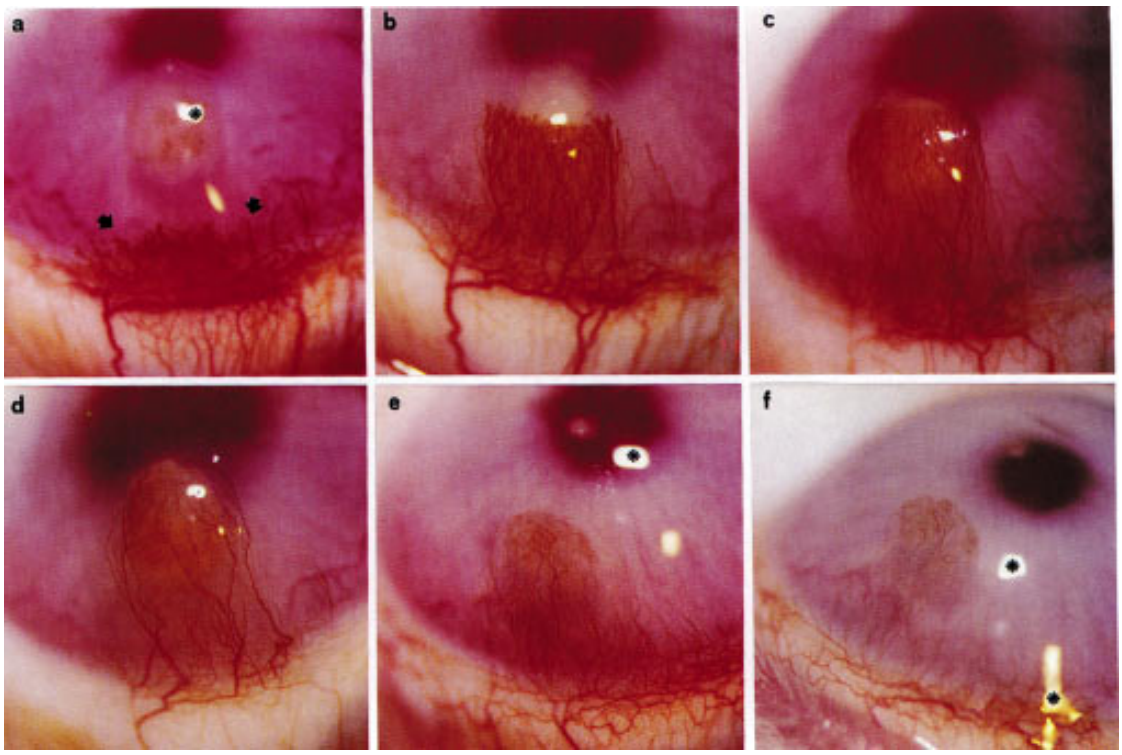

Fig. 5. Angiogenesis induced by tumor samples from head and neck cancer patients in the rabbit cornea: effect of the nitric oxide synthase (NOS) inhibitor N^{ω}-nitro-L-arginine-methyl ester (L-NAME). **Upper panels (a–c):** representative pictures taken at 6, 14, and 24 days, respectively, of neovascular growth produced by a tumor sample in the rabbit cornea. Within 5 days from the surgical implant, the tumor induced a strong neovascular outgrowth at the limbus (**a,** arrows). In the following days (day 14, **b**), angiogenesis induced by the tumor progressed and the newly formed capillaries reached the tumor implant and vascularized it, leading to an increase in the tumor size (day 24, **c**). **Lower panels:** The effect of L-NAME on tumor-induced angiogenesis is shown. L-NAME (1 g/L) was given in the drinking water for 1 week from day 26 after tumor implant. Pictures were taken at 2, 4, and 8 days from the beginning of the treatment. Within 2 days from systemic NOS inhibition, tumor vasculature consistently and progressively regressed **(d–f)** and the tumor size appeared grossly reduced **(e, f).**

occurred within 2 weeks from surgery (Fig. 7, open bars). In rabbits receiving L-NAME, the angiogenic response was reduced and delayed by 1 week (Fig. 7, hatched bars) (Fisher's test following ANOVA, $P = .01$ for days 13–15). When A-431 cells were treated *in vitro* with LPS in the presence of the NOS inhibitor, no angiogenesis was produced by the tumor cells, suggesting that NO production within the tumor cells was required for the angiogenic activity elicited by LPS treatment (Fig. 7, inset).

Discussion

In this study, we show that an increase in NOS activity is found in head and neck cancer, is associated with elevated cGMP levels, and correlates with tumor vascularization. Microvessel density and NOS activity correlate with lymph node metastases, indicating that an increased metastatic behavior is associated with a high NOS activity and angiogenesis. Animal studies demonstrate that transplant of tumor samples and a cell line from squamous cell carcinoma produce angiogenesis *in vivo* strictly linked to NO production, which is made to regress by treatment with NOS inhibitors. Taken together, these data suggest that, in head and neck cancer, the increased NOS activity can be regarded as a novel biologic marker for tumor progression related to angiogenesis and point to inhibitors of NOS as potential antiangiogenic drugs.

Head and neck cancer is a major cause of morbidity and mortality worldwide, representing 5% of all new cancers estimated in major Western countries per year *(1).* The cure rate for head and neck cancer drops substantially when lymph nodes in the neck are involved *(2).* Despite the continuous effort, no reliable prognostic markers for head and neck cancer exist. Angiogenesis is associated with regional and distant tumor spread in several solid tumors, including head and neck cancer *(8–10),* thus predicting patient outcome. Although the microvessel count in tumor tissue correlates with tumor aggressiveness, little information is provided by this pathologic assessment about the biochemical pathway responsible for tumor angiogenesis.

NO has been shown to play a role in various phenomena involved in the angiogenic process. Observations that NOS expression is increased in fresh tumor tissue from gynecologic *(11)* and brain *(33)* neoplasms and that it can be generated *in vitro* by tumor cells *(34,35)* have suggested that NO may have a role in tumor growth and metastasis *(14).* We have recently reported that NO controls angiogenesis by modulating the activity of angiogenic factor released by tumor cells as VEGF *(18,19).*

NOS activity is normally present in the upper and lower airway epithelia, where it plays a major role in host airway

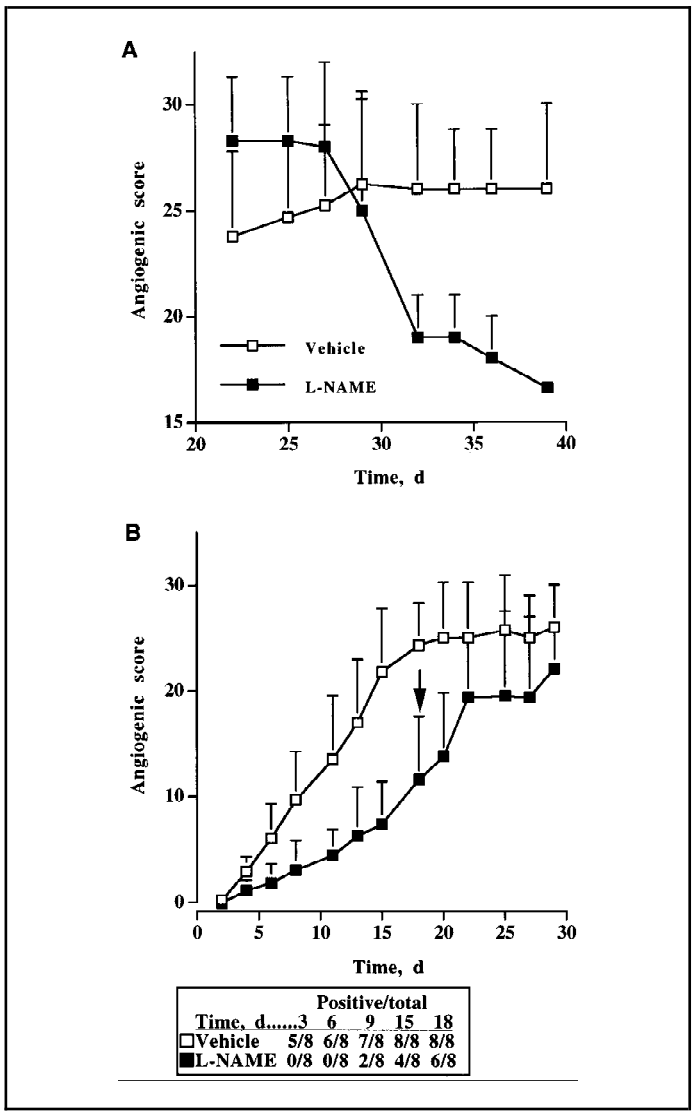

Fig. 6. Effect of the nitric oxide synthase (NOS) inhibitor N^{ω}-nitro-L-arginine-methyl ester (L-NAME) on angiogenesis induced by tumor samples from head and neck cancer patients in the rabbit cornea. **A)** Pattern of regression of tumor-induced angiogenesis by systemic NOS inhibition. L-NAME (1 g/L) was given to the animals in the drinking water for 1 week from day 26 after tumor implant (four fragments from two patients). **B)** Effect of systemic NOS inhibition in preventing tumor angiogenesis. Animals were treated with L-NAME for 1 week before surgery and for 12 days after corneal implant of tumor specimens. Neovascular growth in treated animals did not occur until up to 1 week after treatment discontinuation. The sample size was eight fragments from the tumor of four patients for both of the two experimental animal groups. The efficacy of L-NAME administration was evaluated during and at the end of the treatment as acetylcholine-induced relaxation in rabbit aortic rings preconstricted with phenylephrine as previously described *(27)*. Following 14 days from the beginning of the treatment, the vasorelaxation to 10 μM acetylcholine was 11% (95% confidence interval [CI] = 5%–17%) in L-NAME-treated versus 68% (95% CI = 60%–76%) in aortic rings from untreated animals (10 for each group). After 5 days from the ending of L-NAME administration, vasorelaxation returned to normal levels (40% [95% CI = 34%–46%] relaxation, n = 8) (arrow in **panel B**). d = day.

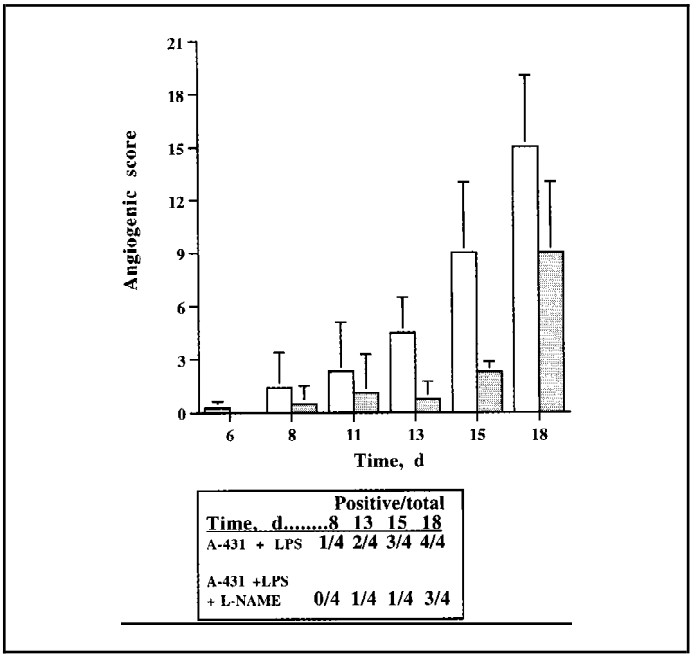

Fig. 7. Angiogenesis induced by A-431 cell line. Angiogenic response of A-431 cells stimulated for 24 hours before corneal implant with 10 μg/mL lipopolysaccharide (LPS) in control animals (open bars) and in rabbits pretreated with L-NAME (dotted bars). Systemic nitric oxide synthase (NOS) inhibition by L-NAME prevented and delayed angiogenesis. Data are expressed as angiogenic score over time (four implants for each experimental group). Table inset: *in vitro* treatment of the cells with 200 μM L-NAME reverted the angiogenic activity of LPS-stimulated A-431 cells. Data are expressed as positive implants over total implants performed (four implants for each experimental group). d = day.

defense mechanism and as a potential mediator of the inflammatory response *(36,37)*. Our results indicate that NOS activity in tumor tissue from patients with head and neck cancer is increased by threefold to fivefold. The rise in iNOS activity is differently distributed within the malignant tissue, being higher at the invasive tumor edge than in the tumor core. The detection of increased NOS/cGMP activity at the tumor front area discloses the heterogeneity of the metabolic demand/function of this signaling cascade within the tumor mass *(38)*. We demonstrate that increases in NOS activity, cGMP levels, and microvessel density are highly correlated with the metastatic phenotype of head and neck cancer at the tumor periphery.

At the interface between tumor and host normal tissue, remodeling of the extracellular matrix and increased angiogenesis take place *(39)*. Multivariate analysis confirms that the intensity of vascularity and cGMP levels at the invasive edge of the tumor correlate independently with the probability of metastasis from the other clinical and biologic features analyzed. Thus, a direct link between increased NOS/cGMP activity and angiogenesis with a more aggressive and metabolically active tumor cell subpopulation can be postulated, indicating a central role of NO production by head and neck cancer in influencing the risk of regional metastasis through neoangiogenesis.

The hypothesis that the increased NOS activity of tumor tissue is a key factor in promoting angiogenesis is demonstrated by the experiment in which tumor fragments are tested in the rabbit cornea. Consistent with angiogenesis being a risk factor for tumor spread, tumor samples from patients with lymph node metastases exhibit a higher angiogenic activity in rabbit corneas. Inhibition of angiogenesis is being proposed as a new approach to control tumor growth and prevent metastasis *(4)*. The angiogenesis induced by head and neck tumor fragments is sensitive to NOS inhibition. Persistent vasodilation is a specific feature in tumor vasculature that also appears to be unresponsive to vaso-

constrictor agents because of increased NOS activity *(40)*. The rapid regression of tumor angiogenesis under systemic NOS inhibition reported here proves that the tumor vasculature in the proliferative state of angiogenesis is highly susceptible to NOS inhibition and regresses. We recently documented that NO sustains endothelial proliferation by inducing the expression of endogenous basic fibroblast growth factor *(29)*. In the presence of NOS inhibition, endothelial cells do not produce basic fibroblast growth factor that can act as a survival factor, possibly modulating apoptosis. Therefore, while NOS inhibition can affect tumor growth by reducing blood flow via vasoconstriction *(41)*, it is also likely that this treatment induces apoptosis in proliferating endothelium by interfering with the autocrine survival mechanism of endothelial cells, ultimately leading to suppression of tumor blood supply. We have demonstrated that the NOS inhibitor L-NAME is able to prevent tumor angiogenesis. In fact, as long as NOS is inhibited in the host tissue, neovascularization is not promoted by the tumor tissue or by the epidermoid cell line. Once the NOS activity is re-established (i.e., released from inhibition) in the host, tumor angiogenesis starts again, suggesting that, like other antiangiogenic drugs, NOS inhibitors require long-term administration to control angiogenesis.

Although a body of evidence indicates a definite role for NO in tumor growth, the end point of increased NO production within the tumor mass is controversial *(42)*. In experimental models, NO facilitates tumor growth and vascularization *(14,43)*. Conversely, increased production of NO by tumor cells causes lysis of bystander cells *(44)*. Our findings suggest that the up-regulation of NOS is a crucial point in the multistep process of head and neck cancerogenesis, being associated with the acquisition of an angiogenic and metastatic phenotype. Although we cannot provide a definite explanation for the mechanism by which NO controls angiogenesis in head and neck cancer, there are suggestive observations. The involvement of the p53 tumor suppressor gene in the regulation of NOS expression *(45)* and angiogenesis *(46)* raises the possibility that the p53 mutation found in approximately 50% of head and neck cancers *(47)* could result in an increase in NO production and, thus, in NO-related angiogenesis, ultimately leading to tumor progression. The existence of a link between VEGF and NO in different biologic settings is also increasingly recognized *(18,19,48)*. VEGF expression correlates with increased vascularity and malignant progression, an event that is likely to occur in head and neck cancer patients *(49,50)*. We recently reported that breast carcinoma cells overexpressing VEGF require the NO pathway to induce angiogenesis *in vivo (19)* and that NO is an upstream signal in the molecular cascade following KDR (kinase domain region) receptor activation in vascular endothelium *(51)*. Thus, NO production by squamous cell carcinoma could possibly control VEGF expression and fate within the tumor.

In conclusion, this study documents that a strong correlation exists between the activity of the NOS pathway, angiogenesis, and metastatic behavior in head and neck cancer. Despite the evidence that assessment of microvessel counts correlates with prognosis in several solid tumors, the pathologic assessment of vascular density does not currently give information about the biochemical pathway involved in tumor angiogenesis and cannot be readily used for monitoring of therapeutic effects or give an overall assessment of angiogenesis. On the basis of the results reported here, we suggest that monitoring NOS activity might provide further information regarding the biologic behavior of head and neck cancer in relation to angiogenesis and tumor spread.

References

(1) Parker SL, Tong T, Bolden S, Wingo PA. Cancer statistics, 1996. CA Cancer J Clin 1996;46:5–27.

(2) Shah JP, Medina JE, Shaha AR, Schantz SP, Marti JR. Cervical lymph node metastasis. Curr Probl Surg 1993;30:1–335.

(3) Folkman J. Angiogenesis in cancer, vascular, rheumatoid and other disease. Nat Med 1995;1:27–31.

(4) Barinaga M. Designing therapies that target tumor blood vessels. Science 1997;275:482–4.

(5) Fidler IJ, Ellis LM. The implications of angiogenesis for the biology and therapy of cancer metastasis. Cell 1994;79:185–8.

(6) Petruzzelli GJ, Snyderman CH, Johnson JT, Myers EN. Angiogenesis induced by head and neck squamous cell carcinoma xenografts in the chick embryo chorioallantoic membrane model. Ann Otol Rhinol Laryngol 1993; 102:215–21.

(7) Lingen MW, Polverini PJ, Bouck NP. Retinoic acid induces cells cultured from oral squamous cell carcinomas to become anti-angiogenic. Am J Pathol 1996;149:247–58.

(8) Gasparini G, Weidner N, Maluta S, Pozza F, Boracchi P, Mezzetti M, et al. Intratumoral microvessel density and p53 protein: correlation with metastasis in head-and-neck squamous-cell carcinoma. Int J Cancer 1993;55: 739–44.

(9) Albo D, Granick MS, Jhala N, Atkinson B, Solomon MP. The relationship of angiogenesis to biological activity in human squamous cell carcinomas of the head and neck. Ann Plast Surg 1994;32;588–92.

(10) Klijanienko J, el-Naggar AK, de Braud F, Rodriguez-Peralto JL, Rodriguez R, Itzhaki M, et al. Tumor vascularization, mitotic index, histopathologic grade, and DNA ploidy in the assessment of 114 head and neck squamous cell carcinomas. Cancer 1995;75:1649–56.

(11) Thomsen LL, Lawton FG, Knowles RG, Beesley JE, Riveros-Moreno V, Moncada S. Nitric oxide synthase activity in human gynecological cancer. Cancer Res 1994;54:1352–4.

(12) Thomsen LL, Miles DW, Happerfield L, Bobrow LG, Knowles RG, Moncada S. Nitric oxide synthase activity in human breast cancer. Br J Cancer 1995;72:41–4.

(13) Rosbe KW, Prazma J, Petrusz P, Mims W, Ball SS, Weissler MC. Immunohistochemical characterization of nitric oxide synthase activity in squamous cell carcinoma of the head and neck. Otolaryngol Head Neck Surg 1995;113;541–9.

(14) Jenkins DC, Charles IG, Thomsen LL, Moss DW, Holmes LS, Baylis SA, et al. Roles of nitric oxide in tumor growth. Proc Natl Acad Sci U S A 1995;92:4392–6.

(15) Moncada S, Palmer RM, Higgs EA. Nitric oxide: physiology, pathophysiology, and pharmacology. Pharmacol Rev 1991;43;109–42.

(16) Nathan C, Xie QW. Nitric oxide synthases: roles, tolls, and controls. Cell 1994;78:915–8.

(17) Schmidt HH, Walter U. NO at work. Cell 1994;78:919–25.

(18) Morbidelli L, Chang CH, Douglas JG, Granger HJ, Ledda F, Ziche M. Nitric oxide mediates mitogenic effect of VEGF on coronary venular endothelium. Am J Physiol 1996;270:H411–5.

(19) Ziche M, Morbidelli L, Choudhuri R, Zhang HT, Donnini S, Granger HJ, et al. Nitric oxide synthase lies downstream from vascular endothelial growth factor-induced but not basic fibroblast growth factor-induced angiogenesis. J Clin Invest 1997;99:2625–34.

(20) International Union Against Cancer. TNM classification of malignant tumours. Berlin: Springer-Verlag, 1987.

(21) Michael L. Squamous cell carcinoma. In: Ferlito A, editor. Surgical pathology of laryngeal neoplasms. London: Chapman & Hall Medical, 1996: 123–42.

(22) Bani D, Masini E, Bello MG, Bigazzi M, Bani Sacchi TB. Relaxin activates the L-arginine-nitric oxide pathway in human breast cancer cells. Cancer Res 1995;55:5272–5.

(23) Ghigo D, Arese M, Todde R, Vecchi A, Silvagno F, Costamagna C, et al.

Middle T antigen-transformed endothelial cells exhibit an increased activity of nitric oxide synthase. J Exp Med 1995;181:9–19.
(24) Weidner N, Semple JP, Welch WR, Folkman J. Tumor angiogenesis and metastasis—correlation in invasive breast carcinoma. N Engl J Med 1991; 324:1–8.
(25) Ziche M, Gullino PM. Angiogenesis and neoplastic progression *in vitro.* J Natl Cancer Inst 1982;69:483–7.
(26) Ziche M, Alessandri G, Gullino PM. Gangliosides promote the angiogenic response. Lab Invest 1989;61:629–34.
(27) Ziche M, Morbidelli L, Masini E, Amerini S, Granger HJ, Maggi CA, et al. Nitric oxide mediates angiogenesis *in vivo* and endothelial cell growth and migration *in vitro* promoted by substance P. J Clin Invest 1994;94: 2036–44.
(28) Chomczynski P, Sacchi N. Single-step method of RNA isolation by acid guanidinium thiocyanate-phenol-chloroform extraction. Anal Biochem 1987;162:156–9.
(29) Ziche M, Parenti A, Ledda F, Dell'Era P, Granger HJ, Maggi CA, et al. Nitric oxide promotes proliferation and plasminogen activator production by coronary venular endothelium through endogenous bFGF. Circ Res 1997;80:845–52.
(30) Reiling N, Ulmer AJ, Duchrow M, Ernst M, Flad HD, Hauschildt S. Nitric oxide synthase: mRNA expression of different isoforms in human monocytes/macrophages. Eur J Immunol 1994;24:1941–4.
(31) Ignarro LJ. Signal transduction mechanisms involving nitric oxide. Biochem Pharmacol 1991;41:485–90.
(32) Franchi A, Gallo O, Boddi V, Santucci M. Prediction of occult neck metastases in laryngeal carcinoma: role of proliferating cell nuclear antigen, MIB-1, and E-cadherin immunohistochemical determination. Clin Cancer Res 1996;2:1801–8.
(33) Cobbs CS, Brenman JE, Aldape KD, Bredt DS, Israel MA. Expression of nitric oxide synthase in human central nervous system tumors. Cancer Res 1995;55:727–30.
(34) Villiotou V, Deliconstantinos G. Nitric oxide, peroxynitrite and nitrosocompounds formation by ultraviolet A (UVA) irradiated human squamous cell carcinoma: potential role of nitric oxide in cancer prognosis. Anticancer Res 1995;15:931–42.
(35) Jenkins DC, Charles IG, Baylis SA, Lelchuk R, Radomski MW, Moncada S. Human colon cancer cell lines show a diverse pattern of nitric oxide synthase gene and nitric oxide generation. Br J Cancer 1994;70: 847–9.
(36) Green SJ. Nitric oxide in mucosal immunity [published erratum appears in Nat Med 1995;1:717]. Nat Med 1995;1:515–7.
(37) Guo FH, De Raeve HR, Rice TW, Stueher DJ, Thunnissen FB, Erzurum SC. Continuous nitric oxide synthesis by inducible nitric oxide synthase in normal human airway epithelium *in vivo.* Proc Natl Acad Sci U S A 1995; 92:7809–13.
(38) Heppner GH. Tumor heterogeneity. Cancer Res 1984;44:2259–65.
(39) Dunstan S, Powe DG, Wilkinson M, Pearson J, Hewitt RE. The tumour stroma of oral squamous cell carcinomas show increased vascularity compared with adjacent host tissue. Br J Cancer 1997;75:559–65.
(40) Andrade SP, Hart IR, Piper PJ. Inhibitors of nitric oxide synthase selectively reduce flow in tumor-associated neovasculature. Br J Pharmacol 1992;107:1092–5.
(41) Tozer GM, Prise VE, Chaplin DJ. Inhibition of nitric oxide synthase induces a selective reduction in tumor blood flow that is reversible with L-arginine. Cancer Res 1997;57:948–55.
(42) Vamvakas S, Schmidt HH. Just say NO to cancer? [editorial]. J Natl Cancer Inst 1997:89:406–7.
(43) Takahashi M, Fukuda K, Ohata T, Sugimura T, Wakabayashi K. Increased expression of inducible and endothelial constitutive nitric oxide synthases in rat colon tumors induced by azoxymethane. Cancer Res 1997;57: 1233–7.
(44) Xie K, Huang S, Dong Z, Juang SH, Wang Y, Fidler IJ. Destruction of bystander cells by tumor cells transfected with inducible nitric oxide (NO) synthase gene. J Natl Cancer Inst 1997;89:421–7.
(45) Forrester K, Ambs S, Lupold SE, Kapust RB, Spillare EA, Weinberg WC, et al. Nitric oxide-induced p53 accumulation and regulation of inducible nitric oxide synthase expression by wild-type p53. Proc Natl Acad Sci U S A 1996;93:2442–7.
(46) Dameron KM, Volpert OV, Tainsky MA, Bouck N. Control of angiogenesis in fibroblasts by p53 regulation of thrombospondin-1. Science 1994; 265:1582–4.
(47) Gallo O, Chiarelli I, Bianchi S, Calzolari A, Porfirio B. Loss of the p53 mutation after irradiation is associated with increased aggressiveness in recurred head and neck cancer. Clin Cancer Res 1996;2:1577–83.
(48) Tsurumi Y, Murohara T, Krasinski K, Chen D, Witzenbichler B, Kearney M, et al. Reciprocal relation between VEGF and NO in the regulation of endothelial integrity. Nat Med 1997;3:879–86.
(49) Sauter E, Nesbit M, Herlyn M. Vascular endothelial growth factor (VEGF) is a marker of disease progression in head and neck cancer [abstract]. Proc Am Assoc Cancer Res 1997;38:331.
(50) Inoue K, Ozeki Y, Saganuma T, Sugiura Y, Tanaka S. Vascular endothelial growth factor expression in primary esophageal squamous cell carcinoma. Association with angiogenesis and tumor progression. Cancer 1997; 79: 206–13.
(51) Parenti A, Morbidelli L, Cui XL, Douglas JG, Hood JD, Granger HJ, et al. Nitric oxide is an upstream signal of vascular endothelial growth factor-induced extracellular signal-regulated kinase$_{1/2}$ activation in postcapillary endothelium. J Biol Chem 1998;273:4220–6.

Notes

O. Gallo and E. Masini contributed equally to this work.

Supported by funds from the Italian Association for Cancer Research (Special Project ''Angiogenesis'') (M. Ziche), European Communities BIOMED-2(''Angiogenesis and Cancer'') (M. Ziche), the National Council of Research (M. Ziche and E. Masini), and the Italian Ministry of University, Scientific and Technological Research (M. Ziche).

We thank Professor D. Bani, University of Florence, for conducting the immunofluorescence analysis and Professor V. Boddi, University of Florence, for doing the statistical evaluation.

Manuscript received October 30, 1997; revised February 10, 1998; accepted February 13, 1998.